

## CRITICAL PARAMETERS OF DUCTILE FRACTURE

M. U. Biel<sup>†</sup>; L. Gołaski<sup>++</sup>

The ductile fracture process of cast steels has been investigated under triaxial stress conditions. The influence of stress state on mechanical properties of tested materials was analysed. A stress criterion of ductile fracture conditioned by structure of materials has been postulated. The ductile brittle transition takes place when cleavage fracture stress is exceeded independently of the amount of plastic deformation.

INTRODUCTION

It is generally believed that crack initiation occurs when a critical value of parameter controlling fracture is exceeded over some microstructurally determined distance. For brittle fracture the cleavage fracture stress is assumed as the critical parameter. This criterion has been confirmed by a number of experiments. However the critical parameter of ductile fracture is still discussed. MacKenzie et al. (1) suggest that the ductile fracture occurs under critical effective plastic strain condition while Mutoh (2) is of the opinion that the critical equivalent stress controls the ductile crack initiation for high strength steels. The investigations on a low carbon cast steel, performed by Biel (3), have been shown that the ductile failure occurs under critical ductile fracture stress condition.

This paper aims at a further study of ductile fracture criterion. It was assumed that the critical parameter of fracture should be independent of the state of stress determined by the stress triaxiality factor  $\sigma_m/\bar{\sigma}$ .

MATERIALS

To avoid the influence of elongated inclusions on frac-

<sup>†</sup> Foundry Research Institute, Cracow, Poland

<sup>++</sup> Technical University of Kielce, Kielce, Poland

ture process the tests have been made on cast steels.

Table 1 - The chemical composition of tested materials in weight per cent

Mate- rial	C	Si	Mn	P	S	Ni	Cr	Mo
G	0,21	0,30	0.98	0.019	0.022	-	-	-
N	0.18	0.48	0.95	0.021	0.020	3.90	-	-
H	0.16	0.61	0.82	0.015	0.021	3.96	1.09	0.47

The materials underwent different heat treatment. The mark I denotes materials with the ferritic pearlitic structure while marks II and III denote materials with predominately temper bainitic structure.

#### INVESTIGATION OF FRACTURE PROCESS

The tests have been made on round circumferentially notched tensile specimens. To vary the state of stress four different notch radii were used. Smooth samples were considered too. Thus five stress triaxiality factors in the range of 0.33 to 1.3 were obtained. The assumed critical load was equal to the beginning of load instability. Using Bridgman (4) solution the axial stress  $\sigma_z$  and equivalent stress  $\bar{\sigma}$  at critical load were calculated. In addition for G and H cast steels the cleavage fracture stress  $\bar{\sigma}_f$  at liquid nitrogen temperature was determined. The centres of fracture surfaces, i.e. the places of the highest stress triaxiality were analysed by means of SEM. Some of the fracture surfaces of the cast steel G and H for different triaxiality factors are given in Figs. 1 and 2.

#### RESULTS AND DISCUSSION

The dependence of axial stress  $\sigma_z$  and equivalent stress  $\bar{\sigma}$  at fracture on the stress triaxiality factors have been analysed. Selected results are presented graphically in Figs. 3 to 6. It has been found for tested materials that the changes of tested parameters vs.  $\sigma_m/\bar{\sigma}$  depend on the structure. For ferritic pearlitic cast steel the maximum stress  $\sigma_z$  at fracture is approximately constant for all applied stress triaxiality factors (Fig. 3). For materials with bainitic structure the equivalent stress  $\bar{\sigma}$  appears to be independent of the stress state (Figs. 4 to 6). For all the tested materials the effective plastic strain to fracture was strongly dependent on stress state triaxiality so it

was not taken for further discussion.

The results obtained suggest that in ferritic pearlitic materials the parameter controlling the ductile fracture is the maximum principal stress  $\bar{\sigma}_z$  while the ductile failure of bainitic structures is equivalent stress  $\bar{\sigma}$  controlled. Thus in agreement with the previous assumption the critical parameter of ductile fracture depends on the structure of tested materials.

It is generally known that the ductile fracture occurs as a result of growth and coalescence of voids initiated from inclusions. On the fracture surfaces of the tested materials a number of large deep dimples accompanied by small rather shallow ones can be seen. The large voids can be detected in early stages of plastic deformation. As was shown by Biel (5) their number coincides with the number of MnS inclusions. However the large voids do not coalesce completely but are linked by small voids which grow rapidly leading to fracture. Thus the critical event in ductile fracture seems to be the small void nucleation. These voids cannot be detected by means of metallographic observation even at high magnifications. Their origin is not well known yet and only some presumptions on the problem of microvoid initiation in tested materials can be made.

For ferritic pearlitic cast steel the microvoids may be initiated at small spherical carbides situated inside the ferritic grains. This supposition is supported by the analysis of stress at carbide matrix boundary at fracture using formula given by Argon et al. (6). This stress is independent of stress state (Fig. 3) and its mean value  $1500 \pm 85$  MPa is close to the 1650 MPa for carbide-ferrite boundary fracture (6). The growth of microvoids initiated at carbides may occur in agreement with mechanism proposed by Broeck (7).

The elucidation of the meaning of equivalent stress  $\bar{\sigma}$  as a critical parameter of ductile fracture for bainitic structures is more complicated. However the independence of  $\bar{\sigma}$  of stress state suggests that microvoids may be initiated when intensive slip band is cutting the lamellas of bainite.

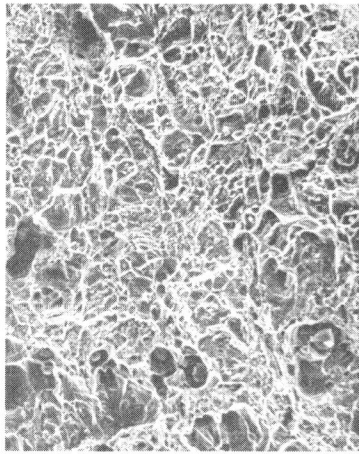
The tested materials fractured generally in a ductile way. The only exceptions is cast steel H II where some cleavage areas in the centre of samples can be seen (Fig. 2). The cleavage has occurred for higher stress triaxiality where maximum principal stress exceeded the cleavage fracture stress  $\bar{\sigma}_f$  as can be seen in Fig. 5.

CONCLUSIONS

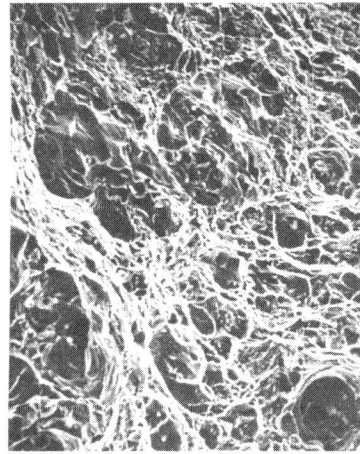
1. The critical parameter controlling the ductile fracture depends on structure.
2. Small voids initiation and coalescence which take place in the first stage of fracture control the fracture process.
3. The brittle fracture occurs when critical cleavage stress is exceeded independently of the amount of plastic deformation.

REFERENCES

- (1) MacKenzie, A.C., Hancock, J.W. and Brown, D.K., Eng. Fract. Mech., Vol. 9., 1977. pp. 167-188
- (2) Mutoh, Y., Eng. Fract. Mech., Vol. 17., 1983. pp. 219-226
- (3) Biel, M.U., ("Mechanism of Ductile Fracture of the Low Carbon Cast Steel"). Proceedings of the ECF 6 Conference on "The Fracture Control of Engineering Structures". Edited by H.C. van Elst and A. Bakker, EMAS, England, 1986.
- (4) Bridgman, P.W., "Studies in Large Plastic Flow and Fracture", McGraw Hill, New York, USA, 1952
- (5) Biel, M.U., ("The Role of Stress Triaxiality and Microstructure in Ductile Fracture of Low Carbon Cast Steel"), Proceedings of the ICM 5 Conference "Mechanical Behaviour of Materials". Edited by Yan, M.G., Pergamon Press, Oxford, England, 1987.
- (6) Argon, A.S. and Im, J., Met. Trans., Vol. 6A., 1975. pp. 839-851.
- (7) Broek, D., Eng. Fract. Mech., Vol. 4., 1973. pp. 9-16.

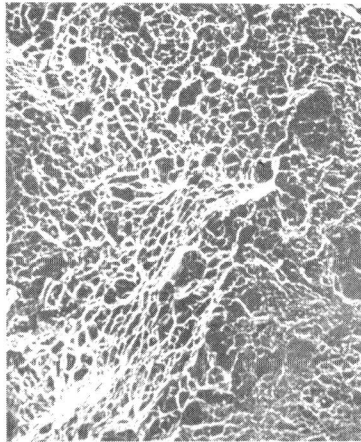


$$\bar{\sigma}_m / \bar{\sigma} = 0.38$$

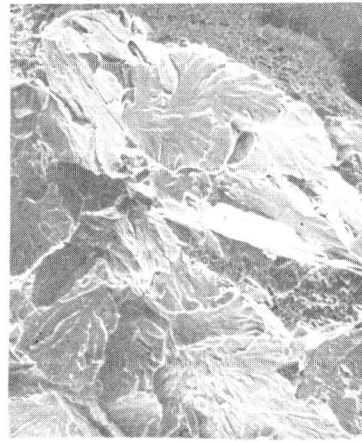


$$\bar{\sigma}_m / \bar{\sigma} = 0.91$$

Fig. 1. Fracture surfaces of G cast steel



$$\bar{\sigma}_m / \bar{\sigma} = 0.54$$



$$\bar{\sigma}_m / \bar{\sigma} = 0.95$$

Fig. 2. Fracture surfaces of H II cast steel

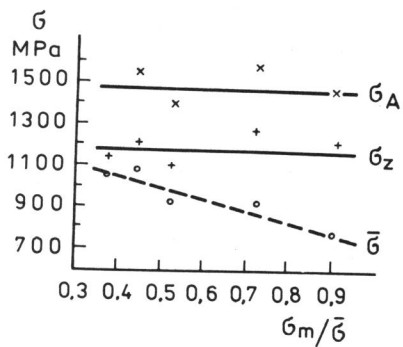


Fig. 3. Fracture data vs.  $\sigma_m/\bar{\sigma}$  cast steel G

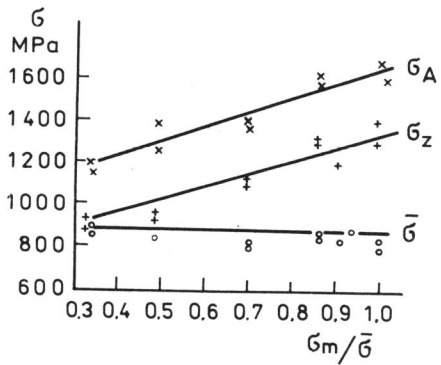


Fig. 4. Fracture data vs.  $\sigma_m/\bar{\sigma}$  cast steel N II

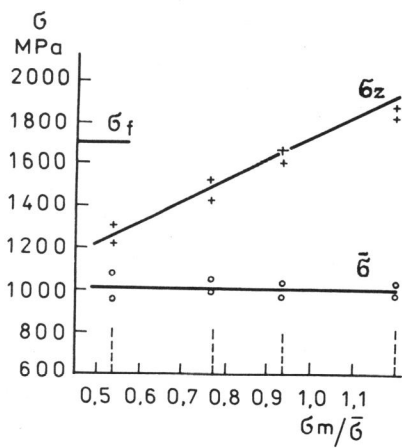


Fig. 5. Fracture data vs.  $\sigma_m/\bar{\sigma}$  cast steel H II

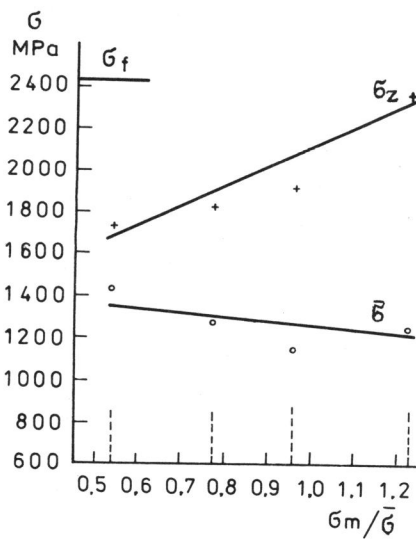


Fig. 6. Fracture data vs.  $\sigma_m/\bar{\sigma}$  cast steel H III